THE JOURNAL OF PHYSICAL CHEMISTRY C LETTERS

2009, *113,* 12943–12945
Published on Web 07/01/2009

On the Role of Pd Ensembles in Selective H_2O_2 Formation on PdAu Alloys

Hyung Chul Ham,[†] Gyeong S. Hwang,*[,†] Jonghee Han,[‡] Suk Woo Nam,[‡] and Tae Hoon Lim[‡]

Department of Chemical Engineering and Institute of Theoretical Chemistry, The University of Texas at Austin, Austin, Texas 78712, and Center for Fuel Cell Research, Korea Institute of Science and Technology, Seoul, Korea

Received: May 11, 2009; Revised Manuscript Received: June 15, 2009

We present the role of Pd ensembles in the selective direct synthesis of H_2O_2 from H_2 and O_2 on a PdAu alloy surface based on periodic density functional theory calculations. Our calculations demonstrate that H_2O_2 formation is strongly affected by the spatial arrangement of Pd and Au surface atoms. In particular, Pd monomers surrounded by less active Au atoms that suppress O−O bond scission are primarily responsible for the significantly enhanced selectivity toward H_2O_2 formation on PdAu alloys compared to that on the monometallic Pd and Au counterparts.

Bimetallic palladium−gold (Pd−Au) alloys have been found to significantly increase catalytic efficiency compared to the monometallic Pd and Au counterparts in various reactions including direct synthesis of hydrogen peroxide (H_2O_2) from hydrogen (H_2) and oxygen (O_2)[1−3] and production of vinyl acetate monomers.[4−6] Recent evidence suggests that the reactivity of bimetallic catalysts can be governed by the creation of unique mixed metal surface sites (the so-called ensemble effect)[7−10] and/or electronic structure change by metal−metal interactions (ligand effect),[11−14] while mechanisms underlying the alloying effect still remain unclear.

It has been reported that Pd monomers surrounded by Au atoms play an important role in boosting catalytic activity for hydrogen evolution,[10] vinyl acetate formation,[5,6] and carbon monoxide adsorption and oxidation.[7] Very recently, the influence of surface Au atoms on the PdAu surface on the direct H_2O_2 synthesis has been studied using density functional theory calculations;[11] yet, detailed reaction mechanisms associated with Pd atomic arrangements are still lacking. In this paper, we present the influence of Pd ensembles on the selectivity of the direct H_2O_2 synthesis based on periodic density functional theory calculations of relevant reaction energetics and pathways.

The calculations reported herein were performed on the basis of spin-polarized density functional theory (DFT) within the generalized gradient approximation (GGA-PW91[15]), as implemented in the Vienna ab initio simulation package (VASP).[16] The projector augmented wave (PAW) method with a plane wave basis set was employed to describe the interaction between the core and valence electrons. The valence configurations employed to construct the ionic pseudopotentials are $5d^{10}6s^1$ for Au, $4d^95s^1$ for Pd, and $2s^22p^4$ for O. An energy cutoff of 350 eV was applied for the plane wave expansion of the electronic eigenfunctions. For the Brillouin zone integration, we used a ($2 \times 2 \times 1$) Monkhorst−Pack mesh of k points to determine the optimal geometries and total energies of the systems examined and increased the k-point mesh size up to ($7 \times 7 \times 1$) to re-evaluate corresponding electronic structures. Reaction pathways and barriers were determined using the climbing image nudged elastic band method (c-NEBM) with eight intermediate images for each elementary step.

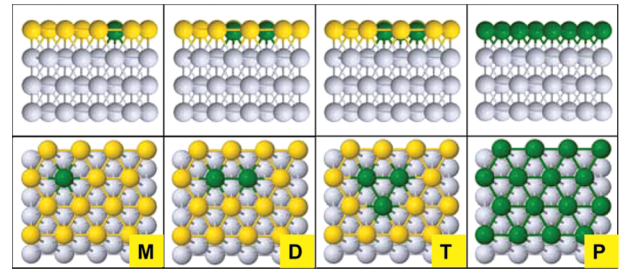

Figure 1. Side (upper panels) and top (lower panels) views of the model PdAu surfaces considered in this work, Pd monomer (indicated as M), dimer (D), trimer (T), and pure (P). The green, gold, and gray balls represent surface Pd, surface Au, and subsurface Pd atoms, respectively.

For a model surface, we used a supercell slab that consisted of a rectangular $2\sqrt{3} \times 4$ surface unit cell with 4 atomic layers, each of which contained 16 atoms (see Figure 1). For each PdAu surface model, the topmost surface layer that was overlaid on a three-layer Pd(111) slab contained a selected Pd−Au alloy [indicated by PdAu/Pd(111) hereafter]. A slab was separated from its periodic images in the vertical direction by a vacuum space corresponding to seven atomic layers. While the bottom two layers of the four-layer slab were fixed at corresponding bulk positions, the upper two layers were fully relaxed using the conjugate gradient method until residual forces on all of the constituent atoms became smaller than 5×10^{-2} eV/Å. The lattice constant for bulk Pd was predicted to be 3.95 Å, which is virtually identical to that from previous DFT-GGA calculations[17] and also in good agreement with the experimental value of 3.89 Å.

As illustrated in Figure 1, in this work, we considered three different Pd ensembles, such as the monomer (indicated by M throughout the paper), dimer (D), and trimer (T), along with pure Pd (P) for comparison purpose. The relative formation

* To whom correspondence should be addressed. Phone: 512-471-4847. Fax: 512-471-7060. E-mail: gshwang@che.utexas.edu.
[†] The University of Texas at Austin.
[‡] Korea Institute of Science and Technology.

10.1021/jp9043545 CCC: $40.75

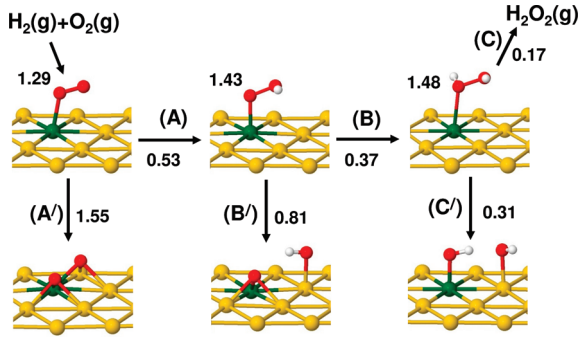

Figure 2. Predicted H_2O_2 formation and competing decomposition steps at a Pd monomer site; (A) O_2 hydrogenation, (A′) O + O scission, (B) OOH hydrogenation, (B′) O + OH scission, (C) H_2O_2 desorption, and (C′) OH + OH scission. Corresponding activation energies (in eV) together with O−O bond lengths (in Å) are indicated. Red, yellow, green, and small white balls indicate O, Au, Pd, and H atoms, respectively. The hydrogenation and decomposition reactions at Pd dimer, trimer, and pure sites are also available in the Supporting Information.

TABLE 1: Calculated Total Energy Changes (ΔE) and Activation Barriers (E_a, in parentheses) for Hydrogenation and Decomposition Reactions with respect to Fully Separated Coadsorbed Species[a,b]

	M	D	T	P
(A)	−0.73	−0.25	0.00	0.18
$O_2 + H \rightarrow OOH$	(0.53)	(0.84)	(0.85)	(0.89)
(A)′	0.25	−0.23	−0.80	−2.08
$O_2 \rightarrow O + O$	(1.55)	(1.54)	(1.05)	(0.51)
(B)	−0.86	−0.51	−0.20	0.09
$OOH + H \rightarrow H_2O_2$	(0.37)	(0.81)	(0.72)	(−)[c]
(B)′	−0.39	−0.92	−1.29	−2.13
$OOH \rightarrow O + OH$	(0.81)	(0.54)	(0.22)	(0.31)
(C)	0.17	0.18	0.21	0.24
$H_2O_2 \rightarrow H_2O_2$ (g)	(0.17)	(0.18)	(0.21)	(0.24)
(C)′	−0.90	−1.35	−1.58	−2.09
$H_2O_2 \rightarrow OH + OH$	(0.31)	(0.11)	(0.08)	(0.01)

[a] The separation state was evaluated by individually placing each adsorbed species on the $2\sqrt{3} \times 4$ unit surface cell employed in this work. [b] All energy values are given in eV. [c] The OOH hydrogenation results in almost spontaneous HO−OH dissociation with no sizable barrier, that is, OOH + H → OH + OH.

energies per Pd atom (E_f) of the Pd monomer, dimer, and trimer are predicted to be 0.07, 0.11, and 0.15 eV, respectively, as given by $E_f = [E_{PdAu} - E_{Au} + N_{Pd}(E_{Au\text{-}bulk} - E_{Pd\text{-}bulk})]/N_{Pd}$, where E_{PdAu}, E_{Au}, $E_{Au\text{-}bulk}$, and $E_{Pd\text{-}bulk}$ represent the total energies of PdAu/Pd(111), Au/Pd(111), bulk Au (per atom), and bulk Pd (per atom), respectively, and N_{Pd} indicates the number of Pd atoms in a given PdAu surface layer. The small formation energy variation with ensemble may imply that Pd atoms could be randomly distributed on the PdAu alloy surface at elevated temperatures, although monomers surrounded by Au atoms are likely to be more energetically favored to a certain degree over dimers and larger clusters. This is consistent with recent studies.[9,18]

As illustrated in Figure 2, H_2O_2 can be produced by two successive O_2 hydrogenation reactions, following a Langmuir−Hinshelwood mechanism.[19] This is possible because of the relative ease of H_2 dissociation on typical metal catalyst surfaces including Pd and PdAu. One could also expect H_2O_2 formation through a combination of two OH radicals, which are generated by O_2 dissociation followed by hydrogenation. However, the combination reaction is energetically unfavorable on both Pd and PdAu surfaces, and also H_2O formation by OH hydrogenation is kinetically more facile.

In addition to the hydrogenation reactions leading to H_2O_2 formation, Pd and PdAu catalysts can be active for O−O bond scission of adsorbed O_2 and OOH, resulting in the formation of H_2O via subsequent hydrogenation of the dissociated O and OH radicals. Moreover, direct dissociation of adsorbed H_2O_2 to H_2O and O (or 2OH) may also take place.[19] Such side reactions will deteriorate the selectivity of H_2O_2 formation. Therefore, we could estimate the performance of chosen catalysts for selective H_2O_2 synthesis from H_2 and O_2 by comparing the energy costs required for H_2O_2 formation and undesirable decomposition reactions.

In this work, we examine three H_2O_2 formation steps and their competing (decomposition) counterparts on Pd and PdAu model surfaces considered (see Figure 1), (1) O_2 hydrogenation [(A)] versus O + O scission [(A)′]; (2) OOH hydrogenation [(B)] versus O + OH scission [(B)′]; and H_2O_2 desorption [(C)] versus OH + OH scission [(C)′]. Table 1 summarizes the predicted total energy changes (ΔE) and activation barriers (E_a) for the hydrogenation and decomposition reactions. The result clearly shows that the reaction energetics and barriers are sensitive to the arrangement of Pd and Au atoms in the PdAu surface layer. Next, we discuss each reaction step.

First, we find that the O_2 binding energy at the top-bridge-top (t-b-t) state (E_b, with respect to the triplet ground state of gas-phase O_2) can substantially decrease on PdAu [E_b = 0.24 (M), 0.64 (D), and 0.75 eV (T)] compared to that on pure Pd(111) (0.95 eV, consistent with 0.89 eV from previous DFT-GGA calculations that employed a smaller surface supercell ($\sqrt{3} \times 2$) and ultrasoft pseudopotentials[17]). Note that for all Pd ensembles considered, we only examined O_2 adsorption at the t-b-t state for the sake of direct comparison, although the top-fcc-bridge (t-f-b) and top-hcp-bridge (t-h-b) states can slightly be energetically more favorable than the t-b-t state in the trimer and pure Pd cases.[17]

Likewise, the amount of charge transferred to the adsorbed O_2 from the surface tends to decrease, albeit to a small degree, that is, 0.30 (M), 0.44 (D, T), and 0.46 e (P), which subsequently leads to a slight change in the O−O bond length [1.29 (M), 1.33 (D, T), and 1.34 Å (P)]. Note that the transferred charge fills the O_2 2p antibonding orbitals and consequently weakens the O−O bond strength. Here, the atomic charge states were estimated using the Bader method,[20] with special care to ensure convergence with respect to charge density grid.

For O_2 dissociation [(A)′], our calculations predict an exothermicity of 2.08 (P), 0.80 (T), and 0.23 eV (D), but on the monomer site, the dissociation reaction turns out to be endothermic by 0.25 eV. Accordingly, the dissociation barrier (in the b-t-b channel) rises from 0.51 (P) to 1.55 eV (M). The significant changes in the reaction energetics are apparently related to the availability of active Pd sites for O_2 adsorption and dissociation.

For the O_2 hydrogenation reaction [(A)], the monomer site turns out to be most favorable, with a barrier of 0.53 eV (which is substantially lower than 0.89 eV on the pure Pd(111) surface). Our calculations also predict that the hydrogenation barriers (0.53−0.85 eV) are sizably lower than the dissociation barriers (1.05−1.55 eV) on the PdAu model surfaces considered, whereas the trend is opposite on the pure Pd surface.

Looking at OOH hydrogenation [(B)] versus O + OH scission [(B)′], only for the monomer case is the hydrogenation barrier (0.37 eV) lower than the scission barrier (0.81 eV). The results demonstrate that the presence of at least an additional adjacent

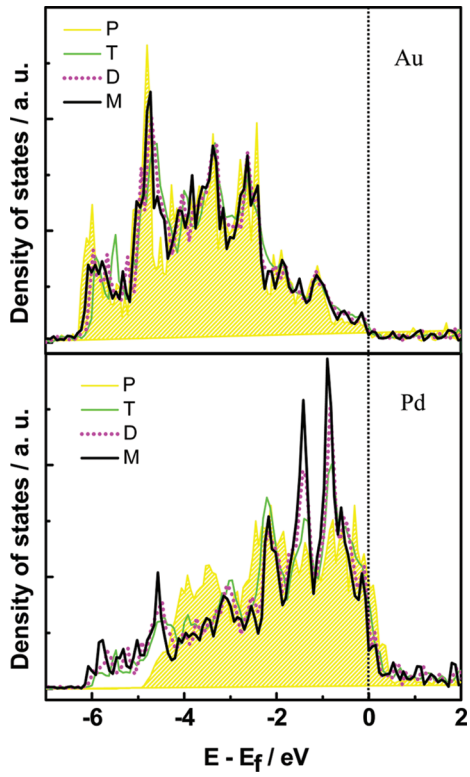

Figure 3. Density of states projected onto the outmost d states of Pd ensembles as indicated (lower panel) and their first nearest Au atoms (upper panel) in the surface layer. The dotted line indicates the Fermi level position.

Pd atom will lead to facile O−OH bond scission. This can be related to the relative binding strength of OOH and dissociated O/OH radicals. The predicted binding energies of O (at a hollow site) and OH (at a top site) noticeably vary with Pd ensemble, that is, for O/OH, 3.43/1.68 (M), 3.87/2.05 (D), 4.21/2.12 (T), and 4.95/2.31 eV (P). On the other hand, the OOH binding energy variation is relatively small, that is, 0.89 (M), 1.03 (D), 1.13 (T), and 1.30 eV (P). This unequivocally demonstrates the importance of Pd atom arrangement on the surface in direct H_2O_2 synthesis with H_2 and O_2.

Provided that H_2O_2 is formed, we finally compared the barriers for H_2O_2 desorption [(C)] versus OH + OH scission [(C)′]. As H_2O_2 desorbs off of the surface, the total energy monotonically increases. The H_2O_2 desorption energies are predicted to vary from 0.17 (M), 0.18 (D), 0.21 (T), to 0.24 eV (P). On the other hand, the barrier for HO−OH bond scission can be as low as 0.1 eV when at least two Pd atoms are located adjacent to each other, indicating that the H_2O_2 dissociation is kinetically more facile than the H_2O_2 desorption. This states that the availability of Pd monomers surrounded by Au atoms will significantly affect the selectivity toward H_2O_2 formation.

To further understand the role played by Pd ensembles in the selective H_2O_2 synthesis, we also calculated the electronic structure of the pure Pd and alloy PdAu model surfaces considered. As summarized in Figure 3, the projected local density of states on surface Pd atoms exhibits a slight shift toward higher binding energy with an increasing number of Au neighbors, that is, Pd d band centers are located at −2.17 (M), −2.13 (D, T), and −2.06 eV (P). There is practically no change with Pd ensemble in the d band center positions of the first nearest Au neighbors, that is, −3.54 (M), −3.49 (D), and −3.46 eV (T), which are slightly lower than −3.59 (M), −3.56 (D), and −3.54 eV (T) for the rest of surface Au atoms. The Au d band center values are, as a whole, close to −3.53 eV for pure Au(111). While the d band center position can be used as a general measure of local surface reactivity, the slight alternations imply that the activity per surface atom has no significant change by the arrangement of surface Pd and Au atoms. This suggests that the large activity difference between Pd and Au atoms may play a major role in determining the selectivity of H_2O_2 formation.

In conclusion, we find that the selectivity of direct H_2O_2 synthesis with H_2 and O_2 will be strongly affected by the arrangement of Pd and Au atoms on a PdAu alloy surface. In particular, the availability of Pd monomers surrounded by less active Au atoms tends to play a key role in enhancing the selectivity toward H_2O_2 formation by suppressing O−O bond scission due to the large activity difference between Pd and Au atoms. For Au-based bimetallic catalysts, this work also hints to the importance of properly tailoring the activity of surface Au atoms in order to achieve desired reactions, while the relative Au activity can be a function of subsurface layer composition as well as catalyst geometry and topology.

Acknowledgment. This work is supported by the Welch Foundation (F-1535). The authors also thank the Texas Advanced Computing Center for use of their computing resources.

Supporting Information Available: Predicted reaction steps for H_2O_2 formation and competing decomposition at the Pd dimer, trimer, and pure surface. This material is available free of charge via the Internet at http://pubs.acs.org.

References and Notes

(1) Edwards, J. K.; Carley, A. F.; Herzing, A. A.; Kiely, C. J.; Hutchings, G. J. *Faraday Discuss.* **2008**, *138*, 225–239.
(2) Abate, S.; Centi, G.; Melads, S.; Perathoner, S.; Pinna, F.; Strukul, G. *Catal. Today* **2005**, *104*, 323–328.
(3) Samnata, C. *Appl. Catal., A* **2008**, *350*, 133–149.
(4) Allison, E. G.; Bond, G. C. *Catal. Rev.* **1972**, *7*, 233–289.
(5) Chen, M.; Kumar, D.; Yi, C.-W.; Goodman, D. W. *Science* **2005**, *310*, 291–293.
(6) Yi, C.-W.; Luo, K.; Wei, T.; Goodman, D. W. *J. Phys. Chem. B* **2005**, *109*, 18535–18540.
(7) Maroun, F.; Ozanam, F.; Magnussen, O. M.; Behm, R. J. *Science* **2001**, *293*, 1811–1814.
(8) Liu, P.; Norskov, J. K. *Phys. Chem. Chem. Phys.* **2001**, *3*, 3814–3818.
(9) Yuan, D.; Gong, X.; Wu, R. *Phy. Rev. B,* **2007**, *75*, 233401.
(10) Pluntke, Y.; Kibler, L. A.; Kolb, D. M. *Phys. Chem. Chem. Phys.* **2008**, *10*, 3684–3688.
(11) Staykov, A.; Kamachi, T.; Ishihara, T.; Yoshizawa, K. *J. Phys. Chem. C* **2008**, *112*, 19501–19505.
(12) Ruan, A.; Hammer, B.; Stoltze, P.; Skriver, H. L.; Norskov, J. K. *J. Mol. Catal. A: Chem.* **1997**, *115*, 421–429.
(13) Sakong, S.; Mosch, C.; Grossa, A. *Phys. Chem. Chem. Phys.* **2007**, *9*, 2216–2225.
(14) Venezia, A. M.; Parola, V. La.; Nicloli, V.; Deganello, G. *J. Catal.* **2002**, *212*, 56–62.
(15) Perdew, J. P.; Wang, Y. *Phys. Rev. B* **1992**, *45*, 13244.
(16) Kresse, G.; Furthmuller, J. *VASP, the guide*; Vienna University of Technology: Vienna, Austria, 2001.
(17) Eichler, A.; Mittendorfer, F.; Hafner, J. *Phys. Rev. B* **2000**, *62*, 4744–4755.
(18) Boscoboinik, J. A.; Plaisance, C.; Neutrock, M.; Tysoe, W. T. *Phys. Rev. B* **2008**, *77*, 045422.
(19) Edwin, N. N.; Edwards, J. K.; Carley, A. F.; Lopez-Sanchez, J. A.; Moulijn, J. A.; Herzing, A. A.; Kiely, C. J.; Hutchings, G. J. *Green Chem.* **2008**, *10*, 1162–1169.
(20) Sanville, E.; Kenny, S. D.; Smith, R.; Henkelman, G. *J. Comput. Chem.* **2007**, *28*, 899–908.

JP9043545